

Chapter 3

Surface Modification of Graphene Nanoplatelets (GNP) Towards Preparation of Natural/Synthetic Rubber Blend Nanocomposites



Ruey Shan Chen, Jeefferie Abd Razak, Noraiham Mohamad,
and Sahrim Ahmad

3.1 Introduction

Inorganic materials are established for reinforcement in polymer composites. In the development of polymer nanocomposites (reinforced with nanofillers), nanoscopic inorganic particles (typically 1–10 nm in at least one dimension) are incorporated in a polymeric matrix with the ideal exfoliation level of nanofiller dispersion. Nanoparticles rubber composites play a vital role in rubber technology and material engineering (Konar et al. 2010). Lately, high-performance elastomer nanocomposites with the reinforcement of various kinds of inorganic nanofillers such as layered silicates, silica nanoparticles, multi-walled carbon nanotubes, etc. have been produced (Li et al. 2017). Graphene is well-known to have exceptional physical and chemical properties, and has been widely applied in electronic devices, adsorption, sensors, energy and conversion, and composites. In the field of composites, graphene serves as multifunctional nanofiller to enhance the mechanical performance, conductivity characteristics in terms of thermal and electrical aspects as well as barrier effect (for instance, gas impermeability) of composites (Bhattacharya 2016). The reinforcing (normalized modulus) mechanism of graphene in elastomers nanocomposite depends on the aspect ratio (filler geometry), volume fraction and orientation of the graphene filler (controlled by the processing methods) but it is independent of the filler modulus (Liu et al. 2018).

R. S. Chen (✉) · S. Ahmad

Materials Science Program, Department of Applied Physics, Faculty of Science and Technology, Universiti Kebangsaan Malaysia, Bangi, Selangor, Malaysia
e-mail: chen@ukm.edu.my

J. A. Razak · N. Mohamad

Advanced Manufacturing Centre, Fakulti Kejuruteraan Pembuatan, Universiti Teknikal Malaysia Melaka, Melaka, Malaysia

© Springer Nature Switzerland AG 2020

S. Siddiquee et al. (eds.), *Composite Materials: Applications in Engineering, Biomedicine and Food Science*, https://doi.org/10.1007/978-3-030-45489-0_3

In this chapter, a focus is made on the natural rubber/ ethylene-propylene-diene-monomer (NR/EDPM) blend matrix reinforced with graphene nanoplatelets (GNP) with different surface modification and nanofiller loading.

3.1.1 Graphene Nanoplatelets

Graphene nanoplatelets (GNP) is discs-shaped graphite particles in a nanometer-sized scale, which comprised of two-dimensional (2D) layers of sp²-hybridized carbon atoms in one-atom thickness that are arranged in a honeycomb hexagonal lattice structure (Chen et al. 2018). GNP made of multiple layers of graphene which corresponds to partially exfoliated graphite. In comparison to monolayer graphene, GNP with various particle sizes are commercially produced at a large scale through top-down methods at a relatively low cost (Zhang et al. 2016). Generally, GNP have an ultimate strength of 130 GPa, a high specific area of 2600 m²/g as well as very high electric conductivity (6000 S/cm) and thermal conductivity above 5000 W m K⁻¹ (Bhattacharya 2016). Therefore, the extraordinary properties of GNP as well as their ultrahigh aspect ratio (600–10,000) and large surface contact area with polymer have resulted this platelet nanomaterial as an ideal reinforcing and multi-functional fillers for polymer nanocomposites (PNC) (Kuan et al. 2018). The platelet's shape promotes higher tortuosity path for molecular transport which further provides the barrier effect to the resultant PNC (Abd Razak et al. 2015b).

The overall reinforcement of GNP in a polymeric matrix is strongly dependent upon its dispersion state and the nanofiller-matrix interfacial interaction. Nevertheless, GNP has a smooth, chemically inert and hydrophobic surface, which these inherent characteristic makes GNP not compatible with many polymers and a weak interfacial bonding is caused (Zhang et al. 2016). The dispersion of GNP in polymer matrices and interface quality control are very challenging because of their strong interlayer cohesive energy and surface inertia (Zhao et al. 2018). This renders GNP tends to easily agglomerate and re-stacking into graphite via van der Waals interactions as it is unable to repel the attractive forces between them as a result of the deficiency of intrinsic functional groups (Abd Razak et al. 2015a).

3.1.2 Surface Modification

Graphene based materials are difficult to achieve intercalation by huge species like polymer chains. In order to enhance the compatibility of GNP with various polymer matrices, the surface modification of GNP could be achieved through either covalent or noncovalent functionalization approaches (Mohamad et al. 2017). Covalent modification or treatment is critically susceptible to destroy the intrinsic properties of graphene, whereas non-covalent treatment ordinarily preserves the pristine structure as well as the intrinsic electrical and thermal conductivities of graphene (Abd

Razak et al. 2015b). The covalent functionalization involves hybridization of one or more sp² carbon atom to sp³ configuration, followed by simultaneous loss of electronic conjugations (Ijeomah et al. 2017). The covalent functionalization of graphene will not only increase the dispersion of GNP, but also increase the graphene-polymer interfacial interaction. GNP typically has a hydroxyl functional group on base and edge section where this hydroxyl group will be hydrated with silane coupling agents with the presence of certain catalyst (Wang et al. 2012). By applying this idea, the silane coupling agent, for instance, aminopropyltriethoxysilane (ATPS), can be act as a chemical bridge to link covalently with polymer matrices chains (Kuila et al. 2012). This covalent approach is proven to serve as an effective method in improving the filler-matrix interfacial interactions, and thus increasing the mechanical and thermal performances. However, the covalent bonding is still considered less than satisfactory as a result of the inadequate oxygen functional groups in GNP (Zhang et al. 2016).

On the other hand, non-covalent functionalization basically involves the van der Waals, electrostatic, π - π stacking, and hydrophobic forces, which require the physical adsorption of the corresponding molecules to the surface of GNP (Ijeomah et al. 2017). This approach has been exploited to tailor the interfaces between GNP and the organic media or to control interfaces within GNP network (Eleuteri et al. 2019). Poly(ethyleneimine) (PEI) is a polycationic polymer that is highly water soluble owing to ethylamine repeating units. The layers of GNP are able to gather the active amino groups in PEI for surface modification with some functional groups like carboxyl or epoxy groups (Abd Razak et al. 2015b).

3.1.3 *Natural Rubber and Synthetic Rubber*

A typical elastomer compound is mainly made from long chain molecules as known as the base polymer which contribute the basic physical and chemical properties. There is a small amount of free space which exists between the long chain molecules where this space permits the independent mobility of the elastomeric molecules, and causes the subsequent deformation (Mohamad et al. 2017). Due to the ease of deformation at ambient condition, good resistance to heat, superior flexibility and elongation before breaking, elastomers or rubbers are extensively used in various engineering industrial sectors such as packaging, aerospace, automotive and healthcare (Li et al. 2017). Rubbers possess good energy absorbing and mechanical (elasticity) properties which drive the commercial use of rubbers as polymeric matrices (La et al. 2018).

Natural rubber (NR) is the largest single type rubber which produced from latex, and NR has been extensively studied for practical applications in the field of automotive tires, footwear, gloves and condom (Mohamad et al. 2017; Srivastava and Mishra 2018). This is owing to biodegradability characteristic, and excellent mechanical properties such as high elasticity, cracking resistance and etc. However, for practical uses, the requirement of natural rubber is essential to enhance the

physical and mechanical properties, to promote processability and flexibility in product design, as well as to reduce the production cost (Mohamad et al. 2017). On the other hand, the most common important synthetic rubbers are ethylene-propylene-diene-monomer (EPDM), silicone rubber, acrylonitrile butadiene rubber, styrene butadiene rubber, ethylene vinyl acetate copolymer, and butyl rubber, etc. These synthetic elastomers are manufactured in the purpose to replace or to be combined with NR in making polymeric matrix with superior properties of NR (Srivastava and Mishra 2018).

In recent years, the elastomeric blends of NR and EPDM synthetic rubber have been extensively employed for investigation owing to their excellent heat and ozone resistance as well as superior performance in the tire application (Motaung et al. 2011). It is evident that the low environmental and ozone resistance of the NR can be improved by mixing highly unsaturated NR with the highly saturated and non-reactive EPDM (Alipour et al. 2013). Besides, the blending of high cost EPDM with the low cost NR could suit the economic aspects as the appreciable price difference can be balanced with outstanding performances.

3.2 Materials

The commercial grade of SMR 20 natural rubber (NR) obtained from Mentari Equipment and Project Sdn. Bhd., Malaysia was 0.16 wt.% dirty retained on 44 apertures, 1.00 wt.% ash content, 0.60 wt.% nitrogen, 0.80 wt.% volatile subject, 30 min Wallace rapid plasticity (Po) and 40 min. % of plasticity retention index (PFU). Ethylene propylene diene rubber (EPDM) grade BUNA EPT 9650 was supplied by LANXESS, Pittsburgh, USA with the Mooney viscosity UML (1 + 8) at 150 °C of 60 ± 6 MU, ethylene content of 53 ± 4 wt%, ENB content of 6.5 ± 1.1 wt% with volatile matter ≤ 0.75 wt%, specific gravity of 0.86 and total ash ≤ 0.50 wt% with non-staining stabilizer. Both rubbers were masticated with two-roll mill prior to their use. Other compounding ingredients such as stearic acid, sulphur and zinc oxide were purchased from System/Classic Chemical Sdn. Bhd., and tetramethyl thiuram disulfide (TMTD) from the Aldrich Chemistry, whereas N-cyclohexylbenthiazolyl sulphenamide (CBS) and N-(1,3-Dimethylbutyl)-N'-phenylp-phenylenediamine (6PPD) were supplied by Flexys America, USA. All ingredients were used as received. Graphene nanoplatelets (GNP) in black and gray powder form, grade KNG-150, was purchased from the Xiamen Graphene Technology Co. Ltd., China. It has a bulk density of 0.3 g/cm³, a true density of 2.25 g/cm³, a specific surface area of 40–60 m²/g and a carbon content of >99.5. Aminopropyltrytoxysilane (ATPS) and poly(ethyleneimine) (PEI) were purchased from Sigma-Aldrich and were used without further purification. APTS has a linear formula of $\text{H}_2\text{N}(\text{CH}_2)_3\text{Si}(\text{OC}_2\text{H}_5)_3$, an average molecular weight (Mw) of 221.37 g mol⁻¹ and a density of 0.946 g ml⁻¹ at 25 °C. PEI, in the form of a viscous colorless liquid of branched polymer, has a linear formula of $\text{H}(\text{NHCH}_2\text{CH}_2)_n\text{NH}_2$,

an average molecular weight (M_w) of $25,000 \text{ g mol}^{-1}$ and a density of 1.030 g ml^{-1} at $25 \text{ }^\circ\text{C}$.

3.3 Methods

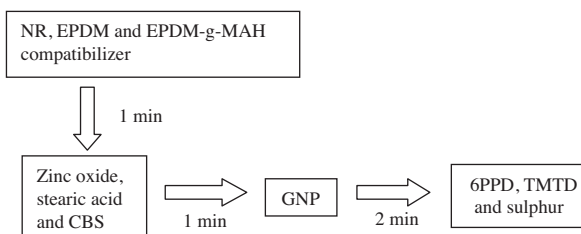
3.3.1 ATPS-Dehydration and PEI-Adsorption of GNP

In this study, both surface treatment of GNP was performed via chemical modification of the exfoliated graphite flakes, which was adapted from Ganguli et al. (Ganguli et al. 2008). The mixture of solvent water: ethanol at the ratio of 25:75 was prepared for every treatment mixture of 2 g GNP and 3 g ATPS or PEI in the 1000 ml of solution mixture. The combination of mechanical stirring using high speed mixer (WiseStir HT50DX) at 1000 rpm and ultrasonication effect using ultrasonic bath set-up (JE10Tech UC-02) at $60 \text{ }^\circ\text{C}$ was performed for 5 hours. Next, the treated GNP was stirred using a hot-plate magnetic stirrer for 100 rpm, $100 \text{ }^\circ\text{C}$ for 45 min. Then, GNP was washed using distilled water as to remove the unreacted chemicals. Further oven heating at $150 \text{ }^\circ\text{C}$ was performed at 5 hrs for complete drying. The dried GNP product was grinded using agate mortar and placed in a close-sealed container.

3.3.2 Preparation of NR/EPDM Rubber Blend Filled GNP Nanocomposites

The compounding process was performed using a Haake Rheomix internal mixer with Banbury rotor type at 0.70 fill factor at 70 rpm of rotor speed and $70 \text{ }^\circ\text{C}$ of blending temperature for about 5 min mixing period. The formulations recipes used in the preparation of NR/EPDM blend were NR/EPDM blend (70,30 phr), EPDM-grafted-maleic anhydride 1.30 phr, 5.0 phr ZnO, 2.0 phr stearic acid, 2.0 phr 6-PPD, 1.0 phr CBS, 0.3 phr TMTD and 1.5 phr sulphur. The percentage of GNP was varied at a 0.00, 0.25, 0.50, 1.00, 3.00, 5.00 wt.%. On mixing procedure (Fig. 3.1), at first, NR, EPDM and EPDM-g-MAH compatibilizer were blended for 1 min before the

Fig. 3.1 Schematic flow of mixing sequence for nanocomposite preparation



first set of curatives consisted of zinc oxide, stearic acid and CBS were added into the internal mixer. After 2 min of mixing, the unmodified or modified GNP was compounded. Next, the second set of curatives consisted of accelerator (6PPD and TMTD) and sulphur were compounded at a minute before end of mixing period. The compound was left to stabilize for 24 hrs before characterization.

3.3.3 Characterization of Unmodified and APTS- and PEI-Modified GNP

Raman spectroscopy and Fourier-transform infra-red (FTIR) spectroscopy analysis were employed to evaluate the success of surface treatment done to the GNP. Raman spectrum was obtained using a Horiba JobinYvon model HR800 with a laser wavelength of 514.53 nm and a laser power at sample of 10 mW. The focal length used was 800 mm with drift amount of $<0.015 \text{ nm sec}^{-1}$. FTIR analysis was performed using JASCO FT/IR 6100 setup at 0.5 cm^{-1} resolution at the range of $4000\text{--}400 \text{ cm}^{-1}$. The morphological evaluation was performed using Field Emission Scanning Electron Micrograph (FESEM, model Hitachi SU8000) at a magnification of 1000 x and a accelerating voltage of 2.0 kV to observe the transformation occurred on modified GNP due to the surface treatment.

3.3.4 Characterization of GNP Filled NR/EPDM Rubber Blend Nanocomposites

The cure characteristics of the blend were studied using MDR 2000 according to the ISO 3417 at $160 \text{ }^\circ\text{C}$. Prior to testing, vulcanizate NR/EPDM based nanocomposites were conditioned for 24 h in a closed container at room temperature. The cure properties such as the scorch time (T_{S2}), maximum curing time (tc_{90}), minimum torque (ML), and maximum torque (MH) as well as cure rate index (CRI). CRI was calculated using the equation as: $\text{CRI} = 100 / (tc_{90} - TS_2)$ (Ahmed et al. 2012).

Tensile tests were conducted using a testometric tensometer Toyoseiki Strogaph-R1 according to ASTM D1822. The dumbbell shaped specimens with the thickness of 2 mm were tested at a crosshead speed of 500 mm/min. At least 7 replicates of each formulation were taken for averaging purposes. The hardness measurements of the nanocomposites were carried out according to ISO 7691 -1 using a manual durometer type Shore A.

Dynamic mechanical thermal analysis was performed on the specimen with a rectangular dimension of 30 mm x 5 mm x 2 mm (length x width x thick) using TA Instruments DMA Q-800. Measurements were carried out from $-100 \text{ }^\circ\text{C}$ to $100 \text{ }^\circ\text{C}$ at a frequency of 5 Hz, amplitude of $15 \text{ }\mu\text{m}$ and heating rate of $5 \text{ }^\circ\text{C}/\text{min}$.

3.4 Results and Discussion

3.4.1 Characterizations of GNP

Figure 3.2 portrays the Raman of unmodified, ATPS- and PEI-modified GNP. It is observed that there are three main characteristic peaks presented at around $1370\text{--}1375\text{ cm}^{-1}$, around $1600\text{--}1610\text{ cm}^{-1}$ and around $2710\text{--}2740\text{ cm}^{-1}$ which are representing D band, G band and 2D band, respectively. It is found that the intensity of the G band and D band for the PEI-modified GNP becomes weaker than that of unmodified GNP. This phenomenon suggests that PEI-treatment results in a higher level of disorder and the formation of defects in the modified graphene layers. As reported in our previous study, G band indicates the intact nature of GNPs' graphitic domain, whereas the D band is a characteristic of defects and disorder (Abd Razak et al. 2015b). The analysis of 2D band peak could examine the arrangement and stacking of GNP layers (Kim et al. 2010). Comparing to unmodified GNP, the intensity of this band peak is lower for ATPS-modified GNP but is higher for PEI-modified GNP. Another strong vibration peak at 2081.11 cm^{-1} is only shown for ATPS-modified (covalent treatment) GNP which attributed to the formation of covalent bonds of C=C bond between the GNP and ATPS.

Besides, the ratio of D band and G band intensity (ID/IG) for ATPS-modified GNP (ID/IG = 0.379) is remarkably increased than those of unmodified GNP (ID/IG = 0.314) and PEI-modified GNP (ID/IG = 0.250). This indicates the transformation of some sp^3 carbon due to the covalent functionalization of GNP after the ATPS

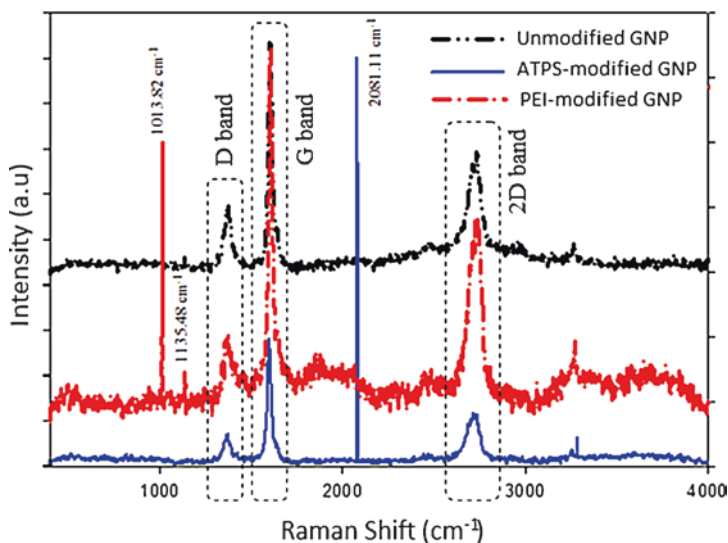


Fig. 3.2 Raman spectra of unmodified, ATPS- and PEI-modified GNP (Part of the work published in (Abd Razak et al. 2015b))

treatment (Fang et al. 2009; Shen et al. 2010). Higher G mode of ATPS-modified GNP than that of untreated GNP confirmed the higher level of disorder for ATPS-modified GNP which relates to random arrangement of GNP layers. These situations might increase the possibilities for molecular chain of rubber into the interlayer space of the intercalated GNP and thus enhance the mechanical interlocking between the rubber blend and the surface of treated GNP for better interfacial interaction. In the case of PEI-modified GNP, the lower ID/IG ratio is corresponded to its high structural integrity caused from PEI treatment (Ma et al. 2014) where this non-covalent treatment done on GNP does not only promotes the disturbance on the arrangement and defects of platelets, but also improves the structure of GNP by physical adsorption.

The FTIR spectra of unmodified, ATPS- and PEI-modified GNP are shown in Fig. 3.3. The presence of absorption band at below $\sim 1000\text{ cm}^{-1}$ for unmodified GNP refers to the presence of trace acid group that intercalates the graphite planes. In comparison to unmodified GNP, the absorption band of 821.08 cm^{-1} is disappeared for ATPS-modified GNP. This implies the possibility of covalent treatment by ATPS occurred through dehydration mechanisms which impedes the presence of minor functional group (C-O). Besides, for ATPS-modified GNP, the shift of C-C stretching of ethyl group ($-\text{CH}_2\text{CH}_3$) at $1060\text{--}1070\text{ cm}^{-1}$ suggests the asymmetric of Si-O-C doublet stretching vibration. These situations confirmed the success of

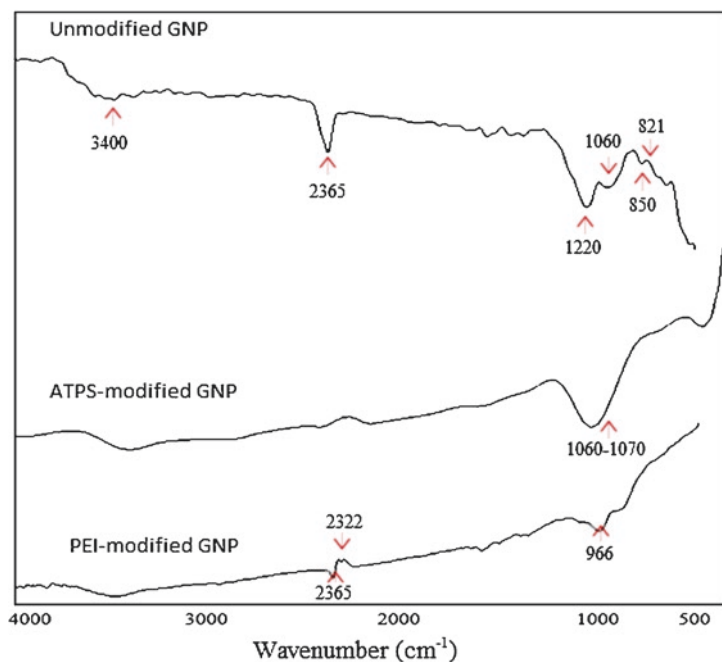


Fig. 3.3 FTIR spectra of unmodified, ATPS- and PEI-modified GNP (Abd Razak et al. 2015a)

covalent (ATPS) modifications on GNP. On the hand, for both unmodified GNP and PEI-modified GNP, there are two distinct peaks at 1069 cm^{-1} and 2365 cm^{-1} which corresponds to the skeletal C–C stretching of ethyl group (or C–O stretching) and the presence of hydroxyl group (–OH stretching), respectively. The FTIR spectrum of PEI-modified GNP displays a new weak band at 966.16 cm^{-1} which corresponds to the skeletal motion of the C–C backbone. This means that the PEI adsorption onto GNP's surface is probably to disturb the arrangement of atomic carbons in the GNP structure (hexagonal lattice) by vibrating to change the dipole moment (Stuart 2005). Also, a new peak at 2322.00 cm^{-1} is existed for PEI-modified GNP and this confirms the interaction between PEI and GNP's surface by forming the hydrogen bonding in the multiple structures of –OH related with the carboxylic acids. The presence of these two new peaks (966.16 cm^{-1} and 2322.00 cm^{-1}) confirms the success of non-covalent modification onto GNP's surface.

Figure 3.4 presents the morphological micrograph of (a) unmodified GNP, (b) ATPS-modified GNP, and (c) PEI-modified GNP. The untreated GNP is not completely exfoliated as the GNP comprises of more than monolayer (Fig. 3.4 (a)). In Fig. 3.4 (b) and (c), a clear separation (increased) interlayer spacing between GNP layers for modified GNP, either ATPS or PEI treatments, in which this confirms the exfoliation nature of modified GNP after undergone the ultrasonication and high-speed mechanical shearing treatment. In comparison to unmodified GNP (control sample), the FESEM micrographs clearly demonstrate the reduction of lateral size but inconsistency in lateral dimension that occurs in ATPS- and PEI-modified GNP. By reducing the dimension of GNP, the cohesive energy between the platelets is reduced and the dispersion of filler in the polymer matrix is improved (Sridhar et al. 2013), as demonstrated in FESEM micrographs.

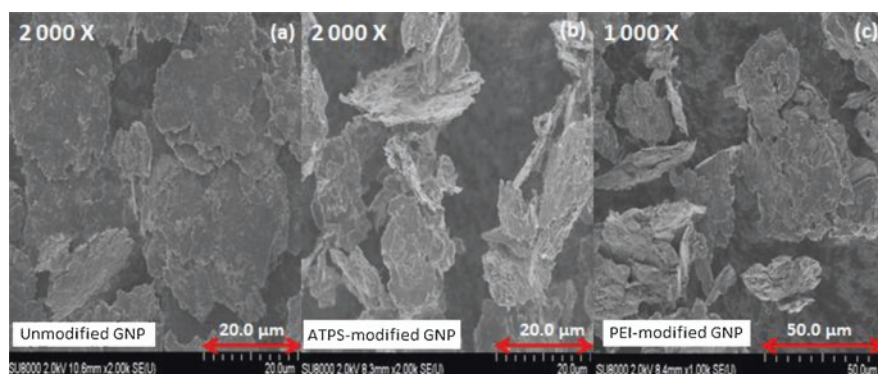


Fig. 3.4 FESEM micrograph of unmodified, ATPS- and PEI-modified GNP (Abd Razak et al. 2015a)

3.4.2 Cure Characterization Studies

The results of scorch time (T_{s2}) with respect of GNP loadings and GNP modifications are plotted in Fig. 3.5. T_{s2} is described as the time required for the state of cure to increase about two torque units higher than the minimum at a given temperature (Nabil et al. 2013). GNP-filled nanocomposites possess a lower scorch safety with an increase of GNP loading than that of the unfilled NR/EPDM blend. However, the NR/EPDM/PEI-modified GNP system has a higher value of T_{s2} than that of NR/EPDM/ATPS-modified GNP system. This means the functionalization of ATPS and the adsorption of PEI polymeric layer onto the surface of GNP tend to improve the interaction between rubber-filler interface, and thus promoting the fast curing of NR/EPDM blend. This phenomenon is due to the high thermal conductivity factor induced by GNP nanomaterial where this has aided in dissipating the heat efficiently and thereby promote the maturation reaction process (Abd Razak et al. 2015b).

Maximum curing time, tc_{90} is defined as the time needed to achieve 90% of full cure where most of the physical properties at this cure state reach their optimum. Figure 3.6 illustrates the tc_{90} of NR/EPDM filled with various loading of unmodified, ATPS-modified GNP, and PEI-modified GNP nanocomposites. It is found that the tc_{90} decreases with the increasing GNP loading for all NR/EPDM blend nanocomposite systems, due to the heat transfer in the nanocomposites is further enhanced by the presence of active GNP filler, thereby encouraging the fulfillment of molds during the vulcanization process. However, NR/EPDM blends incorporated with modified GNP exhibit lower tc_{90} values at all GNP loadings than that of the blends filled with unmodified GNP. This implies that the surface modifications

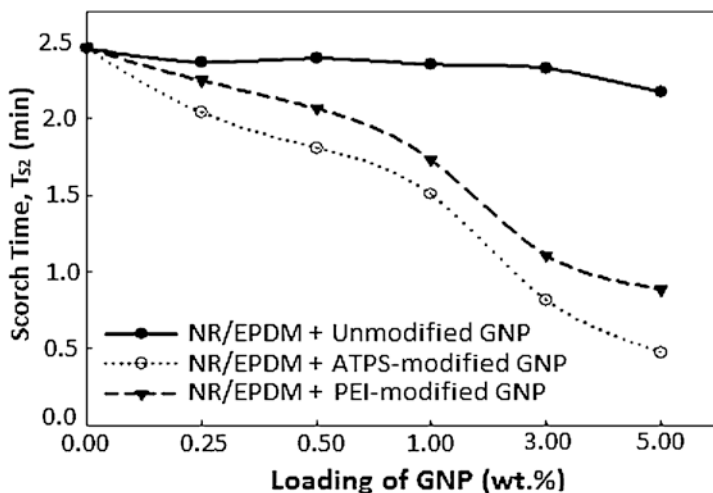


Fig. 3.5 Scorch time (T_{s2}) of NR/EPDM filled with various loading of unmodified, ATPS-modified GNP, and PEI-modified GNP nanocomposites

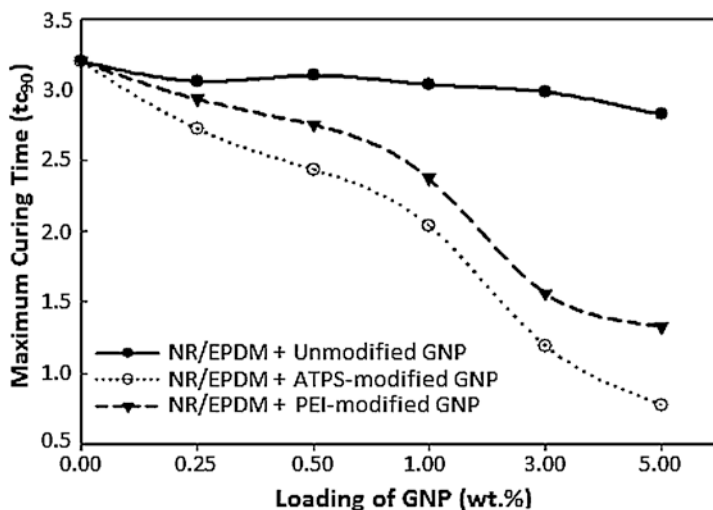


Fig. 3.6 Maximum curing time (t_{c90}) of NR/EPDM filled with various loading of unmodified, ATPS-modified GNP, and PEI-modified GNP nanocomposites

of GNP improve the solubility of GNP with the additional surface chemistry on GNP, and also induce a reduction in their lateral dimension size. These may assist the crosslinking during the vulcanization time for accelerated formation of polysulfide (Konar et al. 2010). Hence, the introduction of ATPS- and PEI-modified GNPs—PEI aids to efficiently cure the NR/EPDM blends with the acceleration of the vulcanization process, as evidence by the reduction of T_{s2} and t_{c90} .

Figure 3.7 and 3.8 show the maximum torque (MH) and maximum torque (ML) of NR/EPDM filled with various loading of GNP in the nanocomposites. MH is the maximum torque that is achieved during the curing time, and is a representative of the vulcanized strength of rubber blend-based compounds or the crosslinking degree in the elastomer. Meanwhile, ML is the minimum torque measured in the rheometer that is often correlated well with the Mooney viscosity of a compound, and ML is an indicator to the uncured stock's elastic modulus. A higher torque obtained indicates the higher number of crosslinks created (Abd Razak et al. 2015b). Overall, the incorporation of modified GNP increases the MH and ML with the increased filler loading. Unlike unmodified GNP, its NR/EPDM blend nanocomposites show a fluctuating pattern and static trend for both MH and ML, respectively, which indicating the less processability of the nanocomposites. From another angle, nanocomposites containing ATPS- and PEI-modified GNP averagely exhibit higher MH and ML values as compared to the one with unmodified GNP. This is attributed to the sufficient filler wetting characteristics resulted from the enhanced filler interaction with NR/EPDM macromolecules network. The addition of modified GNP increases the processing load because of the increased flow resistance that caused by smaller sized GNP as well as the formation of percolation structures by the edge-to-edge and edge-to-face interactions between the dispersed layers. Therefore, this

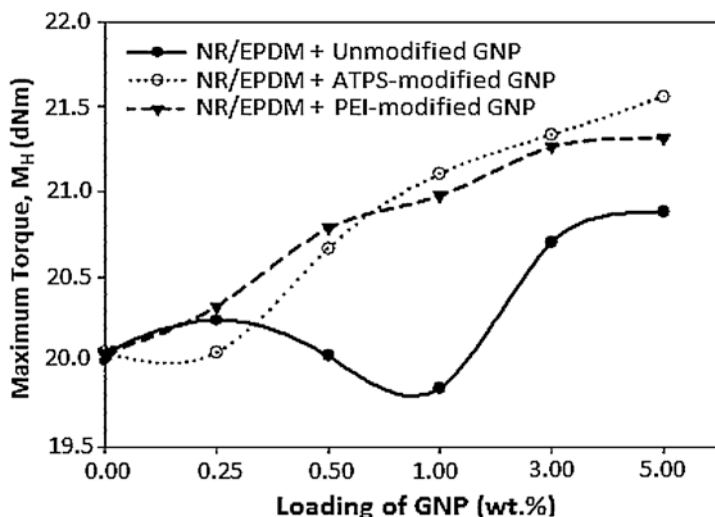


Fig. 3.7 Maximum torque (MH) of NR/EPDM filled with various loading of unmodified, ATPS-modified GNP, and PEI-modified GNP nanocomposites

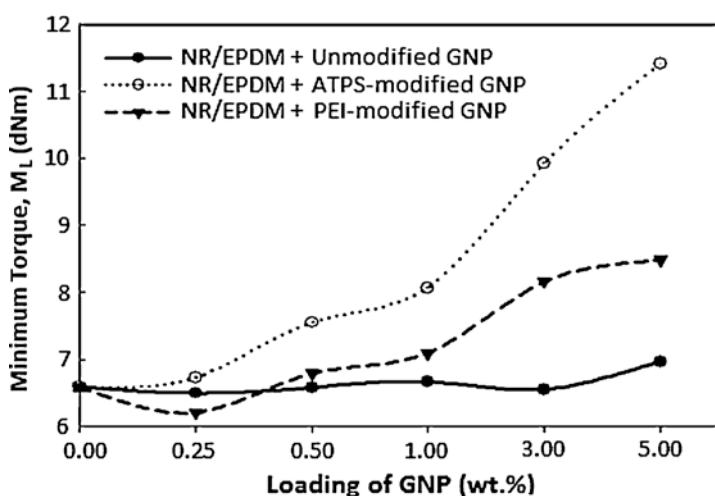


Fig. 3.8 Minimum torque (ML) of NR/EPDM filled with various loading of unmodified, ATPS-modified GNP, and PEI-modified GNP nanocomposites

factor strongly hinders the molecular movement of macromolecules and thus leading to an increase in the processing torque behavior (Konar et al. 2010).

The torque difference (MH – ML), a measurement of the vulcanization extent and accomplishment of a characteristic network chains (Konar et al. 2010), of NR/EPDM nanocomposites filled with various loading of GNP is portrayed in Fig. 3.9. The NR/EPDM nanocomposites filled with unmodified GNP show a uniform

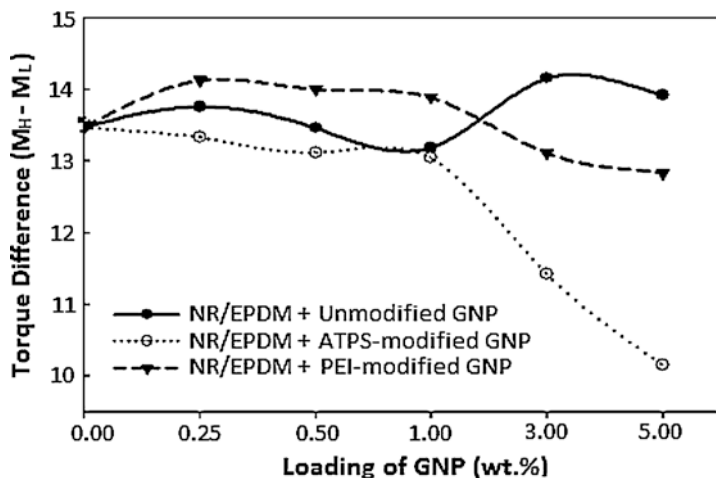


Fig. 3.9 Torque difference (MH – ML) of NR/EPDM filled with various loading of unmodified, ATPS-modified GNP, and PEI-modified GNP nanocomposites

fluctuating plot pattern for the torque difference with the increased loading of unmodified GNP. The fluctuation of MH - ML torque values indicates the possibility of a non-uniform cross-distribution phenomenon because of the incompatible maturation condition between the NR (highly unsaturated) and EPDM (highly saturated) rubber components, thereby resulting in an uneven distribution of crosslink density (Nabil et al. 2013) and inferior mechanical properties of the NR/EPDM filled unmodified GNP. Meanwhile, the nanocomposites filled with modified GNP present a decreasing trend of (MH - ML) values with the increase of GNP loading. The NR/EPDM filled ATPS-modified GNP seems to have a significantly reduced profile as compared to nanocomposites incorporated with PEI-modified GNP at all range of loadings. In the case of PEI-modified GNP nanocomposites, the presence of the PEI polymers absorbed on the surface of GNP has resulted in the disruption of the formation of continuous crosslinks and interactions between the rubber phases in the blends. This is ascribed to the uniform isolation and dispersion of PEI-modified GNP as compared to the unmodified GNP filled nanocomposites. The more the PEI-modified GNP presented, the lower the torque difference value, as a result of the reduced crosslinking formed in the NR/EPDM blend matrices. In contrast, the decline trend for ATPS-modified GNP nanocomposites is insignificant with the GNP loading.

The plot of cure rate index (CRI) versus the GNP loading for three nanocomposite systems is presented in Fig. 3.10. There is no considerable variation observed in the CRI for the unmodified GNP nanocomposite system. When approximately 0.50 wt.% of unmodified GNP was introduced into the NR/EPDM blend, the CRI is found to decrease slightly. This is attributed to cure incompatibility effects resulted from the decrease in reactive sites on the surface of rubber molecules that are available for crosslinking reactions (Nabil et al. 2013). On the other hand, the CRI value

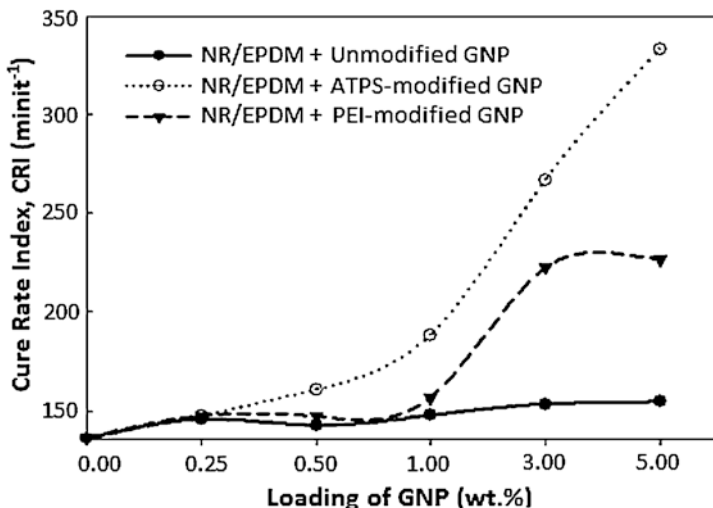


Fig. 3.10 Cure rate index (minit^{-1}) of NR/EPDM filled with various loading of unmodified, ATPS-modified GNP, and PEI-modified GNP nanocomposites

is in line with the increase in the loadings of ATPS- and PEI-modified GNP, which may be associated to the reduction of activation energy for crosslinking process (Tavakoli et al. 2011) and the increased interaction sites for vulcanization (Ahmed et al. 2012) with the presence of these two fillers.

Tensile strength, percentage of elongation, stiffness at 300% elongation (M300) and hardness Shore A of NR/EPDM nanocomposites filled with different loading and types of GNP are shown in Figs. 3.11, 3.12, 3.13, 3.14, respectively. Generally, the results clearly show that the tensile properties are significantly increased with the increase of GNP loading into the NR/EPDM matrices. However, surface modifications performed on GNP has caused the improvement in mechanical properties with the increasing filler loading, up to the certain filler loading, before the occurrence of decline of the improvement rate in tensile results at certain much of filler. By comparing the effect of surface modifications on GNP, nanocomposites filled with ATPS- and PEI-modified GNP experience a slightly improvement in tensile properties as compared to NR/EPDM nanocomposites filled with unmodified GNP at all loadings.

3.4.3 Mechanical Properties

As shown in Fig. 3.11, it is found that the tensile strength drastically increases up to 104–124% when 5.00 wt.% of ATPS- and PEI-modified GNP are added into NR/EPDM blend as compared to the unfilled blend. The maximum improvement of tensile strength obtained by ATPS-modified GNP nanocomposites indicates that the

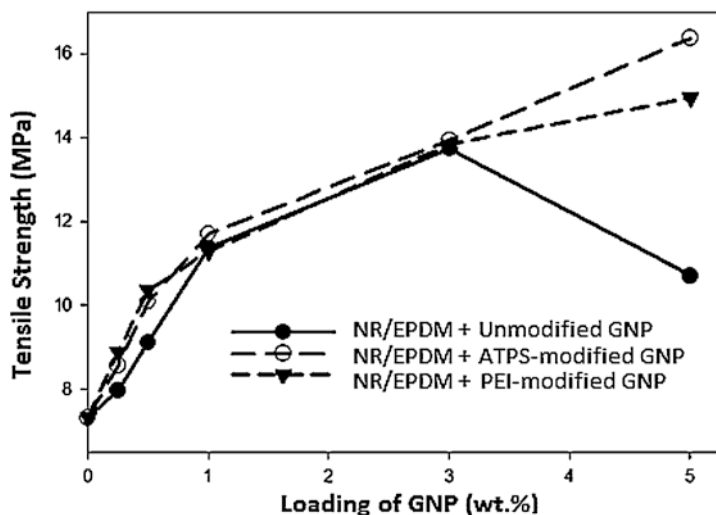


Fig. 3.11 Tensile strength of NR/EPDM filled with various loading of unmodified, ATPS-modified GNP, and PEI-modified GNP nanocomposites

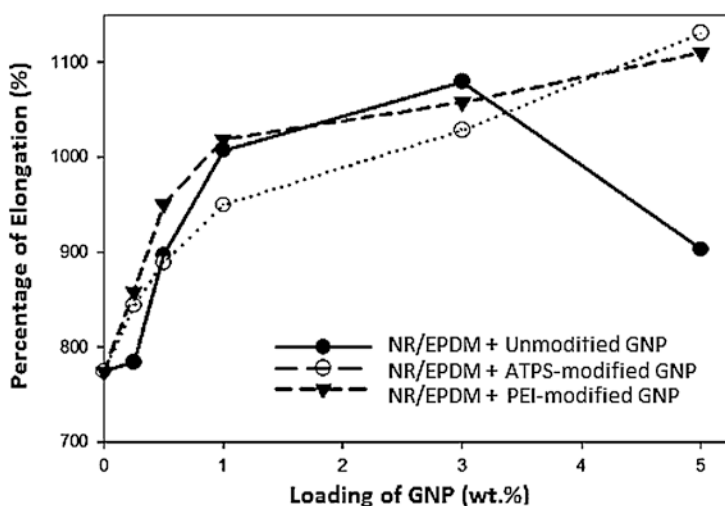


Fig. 3.12 Percentage of elongation of NR/EPDM filled with various loading of unmodified, ATPS-modified GNP, and PEI-modified GNP nanocomposites (Razak et al. 2015; Razak et al. 2014)

covalent treatment aids the separation and intercalation between filler platelets as well as increases the surface wetting (Razak et al. 2014). Surface modification of GNP using PEI treatment succeeds in enhancing the mechanical performance of NR/EPDM blends by creating retention effects among GNP upon the adsorption of the polymeric layer of PEI, and the oxygen-containing groups in the GNP introduce

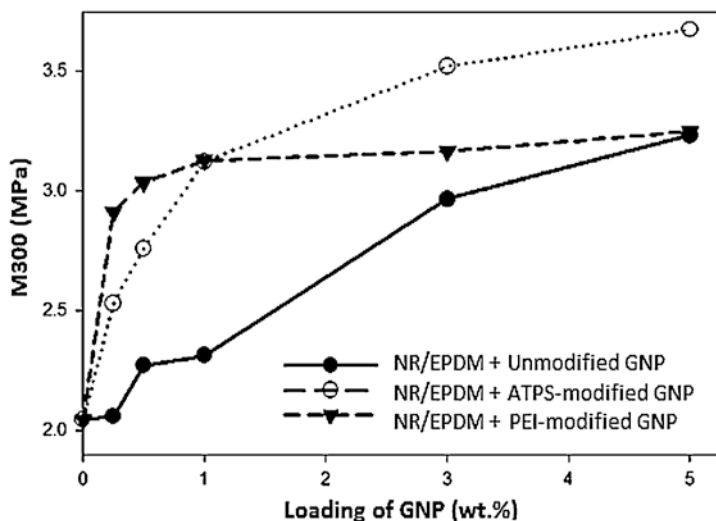


Fig. 3.13 Stiffness at 300% elongation (M300) of NR/EPDM filled with various loading of unmodified, ATPS-modified GNP, and PEI-modified GNP nanocomposites (Razak et al. 2015; Razak et al. 2014)

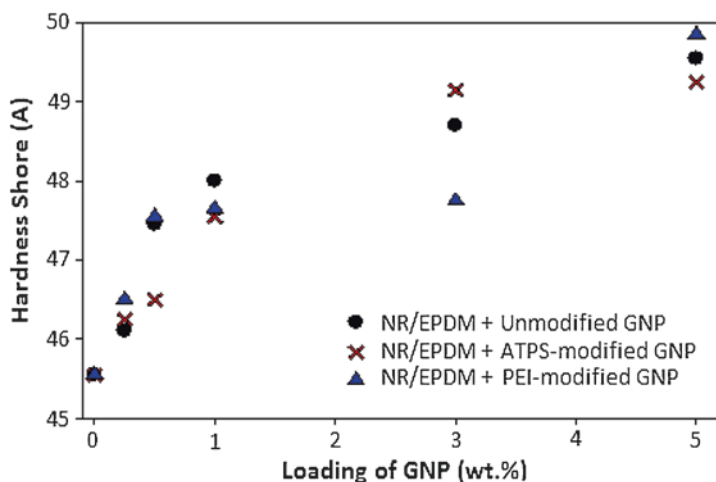


Fig. 3.14 Shore A hardness of NR/EPDM filled with various loading of unmodified, ATPS-modified GNP, and PEI-modified GNP nanocomposites

the polar interactions between PEI-modified GNP sheets and polar polymer matrices, thereby results in the better filler dispersion within the NR/EPDM blend (Zhang et al. 2012). At the same filler loading of 5.00 wt.%, a reduction in tensile strength is encountered for nanocomposite system with unmodified GNP which is due to the agglomeration of GNP that allowing the pre-mature failure (Abd Razak et al. 2015b).

For percentage of elongation in Fig. 3.12, an overall increasing trend is clearly similar to tensile strength. The percentage of elongation increases dramatically with the increase of GNP loading in the NR/EPDM blend matrices. However, this phenomenon only applies to the nanocomposites filled with modified GNP, but not to the nanocomposites with unmodified GNP. Nanocomposites based on the unmodified GNP experience a major decrease in percentage of elongation value due to the induction of some weak points by the agglomeration of GNP in which this facilitates a pre-mature failure when the stress is applied. This suggests poor interfacial interactions and adherence between unmodified GNP and NR/EPDM matrices, and thus probably causes to reduction in the mechanical properties of filled rubber (Arayaprane and Rempel 2008). In the case of ATPS-modified GNP nanocomposites, the elongation values are slightly lower than those of other nanocomposite systems, at the loading of ATPS-modified GNP less than 5.00 wt.%. This situation shows that the interaction of rubber blend matrices with the ATPS-modified GNP is increasing because of the presence of the functional groups that forms the links between the nanofillers and matrices. In which this benefits the improvements of the stiffness properties. For PEI modification, this nanocomposite system has appreciably higher values of the percentage of elongation than the other two nanocomposite systems, for almost all loadings used. This can be ascribed to the even dispersion and distribution of PEI-modified GNP within the rubber blend matrices. Additionally, the physical adsorption of PEI on the GNP's surface is only bonded by the weak van Der Waals and this has increased the capability of GNP and rubber blend macromolecular for slippage. Therefore, the elongation ability is increased (Abd Razak et al. 2015b).

The stiffness at a specific elongation points of 300% (M300) for nanocomposites with various modifications and filler loadings are plotted as shown in Fig. 3.13. Generally, as the nanofiller (with and without surface modification) loading increases, the M300 values are noted to increase nonlinearly. This positive trend is the manifestation of the reinforcement effect imparted by GNP in the NR/EPDM rubber matrices. This finding was in agreement with the previous work reported on other rubber blend systems incorporated with various kinds of filler (Sae-oui et al. 2007; Shehata et al. 2006). In comparison of the surface modification strategies, it is noted that ATPS-modified GNP nanocomposites possesses the highest M300 values, followed by PEI-modified GNP nanocomposites and lastly for nanocomposites filled with unmodified GNP. The improvement for NR/EPDM blend nanocomposites filled with modified GNP is contributed to the lamellar structure of GNP which allowing a better wettability and rubber–nanofiller interactions induced by the hydrogen and van der Waals forces, and hence causing to a better stress transfer (Sridhar et al. 2013).

As observed in Fig. 3.14, Shore A hardness shows an increasing trend with the increase of GNP loading. The hardness value for unfilled NR/EPDM blend is 45.5 and the optimum value up to 49.8 for NR/EPDM blend nanocomposites filled with 5.00 wt.% PEI-modified GNP. The increase in hardness properties is related to the high strength of the resultant nanocomposites (Arroyo et al. 2007). As the value of hardness increases, the higher the amount of crosslinking content found in the blend

matrices, and the more effective reinforcement mechanism introduced by the presence of added GNP fillers. In the aspect of surface modification effects, it is found that at 3.00 wt.% GNP, the trend of Shore A hardness is as follows: NR/EPDM/APTS-modified GNP > NR/EPDM/unmodified GNP > NR/EPDM/PEI-modified GNP.

3.4.4 Dynamic Mechanical Thermal Analysis

Storage modulus (E') refers to the energy stored elastically during deformation, which indicates the elasticity of a material (Chen et al. 2015). Figure 3.15 shows the storage modulus of NR/EPDM-based nanocomposites containing GNP with different surface modifications as a function of temperature. It can be observed that the E' values in the glassy region (around $-50\text{ }^{\circ}\text{C}$) appeared in a sharp peak, following the descending trend as: NR/EPDM/APTS-modified GNP > NR/EDPM/unmodified GNP > NR/EDPM > NR/EDPM/PEI-modified GNP. This finding confirms the efficiency of APTS-modified GNP to act as active filler which provide the reinforcement effect to NR/EPDM (Karger-Kocsis et al. 2010). In the case of non-covalent treatment (with APTS), the addition of GNP had increased the energy stored in the NR/EDPM blend nanocomposites, thereby showing higher E' values. The improvement of E' implies the increased filler/matrix interfacial which thereby reducing the mobility of chains in which caused to the increased stability of nanocomposites with the increasing temperature. Therefore, the E' decreases with the temperature.

Loss modulus (E'') is the energy being dissipated or replaced as heat during the deformation of a material, which is associated with the material's viscous behavior

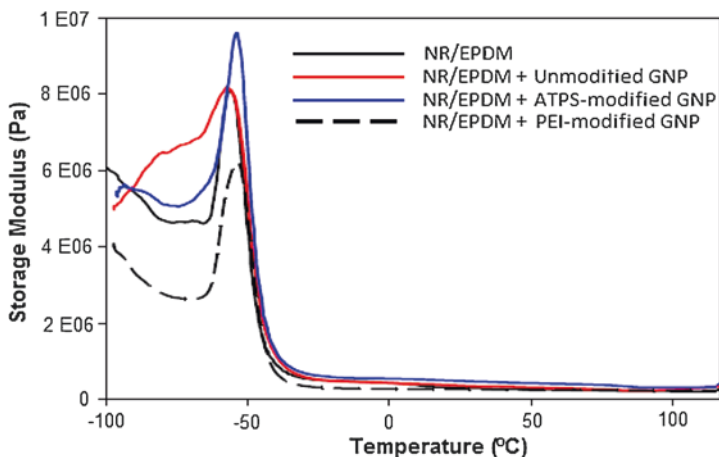


Fig. 3.15 Plots of storage modulus versus temperature for NR/EPDM nanocomposites filled with various modification of GNP

(Part of the work published in (Razak et al. 2017))

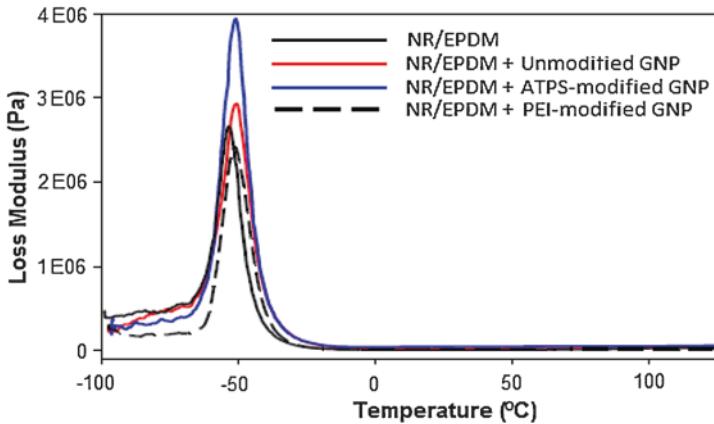


Fig. 3.16 Plots of loss modulus versus temperature for NR/EPDM nanocomposites filled with various modification of GNP (Part of the work published in (Razak et al. 2017))

(Chen et al. 2015). The E'' of NR/EPDM-based materials as a function of temperature is demonstrated in Fig. 3.16. At glass transition temperature, relaxation process allows the greater movement of individual chains in the NR/EPDM blends irrespective of GNP. This can be seen from the highest values of E'' at around $-50\text{ }^{\circ}\text{C}$ in Fig. 3.16. Similarly, the E'' peak for NR/EPDM nanocomposites filled with APTS-modified GNP is higher than that of unmodified GNP. This shows that covalent surface modification of GNP via APTS could increase the heat dissipation characteristics. The lesser heat entrapment in NR/EPDM reinforced with APTS-modified GNP has resulted in the consequent lacking of heat build-up in comparison to other investigated materials. Another reason for the improved E'' in APTS-modified GNP filled NR/EPDM nanocomposites is that APTS-modified GNP improved rubber-filler interface bond strength which is required to activate the immobilization of filler towards the stress transfer in the region of matrix-filler interface. There is another observation shown in Fig. 3.15, the broadening E'' peak is as the following trend: NR/EDPM/APTS-modified GNP > NR/EDPM/unmodified GNP > NR/EDPM = NR/EDPM/PEI-modified GNP. The broaden modulus peak indicates the greater immobilization being introduced onto amorphous phase or molecular chains in NR/EDPM (induced by GNP particles) (Jayalatha and Kutty 2013).

3.4.5 Comparison of Mechanical Properties With Previous Studies

Table 3.1 describes the comparison of mechanical properties with previously reported work on NR/EDPM blend composite materials with different loadings of GNP. Generally, higher values of elongation at break (780–900% for untreated GNP

Table 3.1 Comparison of mechanical properties with previous studies

Matrix	GNP loading, (treatment)	Tensile Strength, MPa	Elongation at break, %	M300, MPa	Shore Hardness, A	Source
NR/ EDPM	0.25 wt.% (unmodified)	8	780	2.1	46	Current study
	(modified)	9 (PEI)	850 (PEI)	2.9 (PEI)	46.5 (PEI)	
	5 wt.% (unmodified)	11	900	3.1	49.5	
	(modified)	16 (APTS)	1100 (APTS)	3.6 (APTS)	50 (APTS)	
NR latex	3% (unmodified)	18–20	600	5	38–45	Charoenchai et al. (Charoenchai et al. 2019)
NR	5 phr 20 phr (unmodified)	18–24 14–23	–	–	56–58 68–72	Li et al. (Li et al. 2017)
Styrene butadiene rubber (S-SBR)	1 phr 25 phr (unmodified)	2.96 7.16	436 464	–	–	Das et al. (Das et al. 2012a; Das et al. 2012b)

and 850–1100% for APTS-modified GNP) are obtained from this study as compared with previous studies on natural rubber/GNP. However, the tensile strength and hardness are found to be comparable (or slightly lower) to the previously published works based on the similar content of GNP. This could be due to the use of NR/EDPM blend as matrix, instead of solely NR as used by previous research, which is likely to improve the elongation characteristic of rubber material.

3.5 Conclusion

This study has shown that covalent and non-covalent surface modifications of GNP with APTS and PEI were successfully performed by a combination method of ultrasonication and high shear mechanical stirring procedure. The nanocomposites were prepared by dispersing the GNP in the NR/EPDM blend using the internal melt mixing procedure, and followed by curing under the semi-EV vulcanization system. A strong vibration band in Raman peak at 2081.11 cm^{-1} which corresponded to the formation of covalent bonds of C=C between the GNP and APTS, as well as the disappearance of 821.08 cm^{-1} in FTIR spectrum confirmed the APTS surface modification mechanism through dehydration. For PEI-modified GNP, the FTIR spectrum presented the presence of a new weak band at 966.16 cm^{-1} which referred to the skeletal motion of the C–C backbone, thus confirming an adsorption of the polymeric PEI into GNPs surface. The increasing GNP nanofiller loading in the NR/EPDM rubber blend promoted the processability of the blend by increasing the T_{s2} and CRI. By adding 5.00 wt.% APTS- and PEI-modified GNP, approximately 124%

and 104% increments in tensile strength were obtained. In term of dynamic mechanical properties, the covalent modification (ATPS-modified GNP) appeared to be more suitable treatment for GNP than non-covalent method in giving the effective improvement. It can be concluded that the incorporation of GNP accelerated the curing process of rubber blend so to reduce the time and cost of the rubber blend vulcanization and product preparation cycle, as well as provided a remarkable improvement in mechanical properties of resultant nanocomposites.

Acknowledgments The authors would like to thank Universiti Kebangsaan Malaysia (UKM) and Universiti Teknikal Malaysia Melaka (UTEM) for financial support under the science fund GUP-2018-107 and PJP/2016/FKP/HI6/S01483.

References

- Abd Razak J et al (2015a) Facile surface modification of Graphene Nanoplatelets (GNPs) using covalent ATPS-dehydration (GNPs-ATPS) and non-covalent Polyetherimide adsorption (GNPs-PEI) method. *Appl Mech Mater* 761:391–396. <https://doi.org/10.4028/www.scientific.net/AMM.761.391>
- Abd Razak J, Haji Ahmad S, Ratnam CT, Mahamood MA, Mohamad N (2015b) Effects of poly(ethyleneimine) adsorption on graphene nanoplatelets to the properties of NR/EPDM rubber blend nanocomposites. *J Mater Sci* 50:6365–6381. <https://doi.org/10.1007/s10853-015-9188-5>
- Ahmed K, Nizami SS, Raza NZ, Shirin K (2012) Cure characteristics, mechanical and swelling properties of marble sludge filled EPDM modified chloroprene rubber blends. *Adv Mater Phys Chem* 2:90. <https://doi.org/10.4236/ampc.2012.22016>
- Alipour A, Naderi G, Ghoreishy MH (2013) Effect of nanoclay content and matrix composition on properties and stress-strain behavior of NR/EPDM nanocomposites. *J Appl Polym Sci* 127:1275–1284. <https://doi.org/10.1002/app.37752>
- Arayapraneew W, Rempel GL (2008) A comparative study of the cure characteristics, processability, mechanical properties, ageing, and morphology of rice husk ash, silica and carbon black filled 75: 25 NR/EPDM blends. *J Appl Polym Sci* 109:932–941. <https://doi.org/10.1002/app.28111>
- Arroyo M, Lopez-Manchado M, Valentin J, Carretero J (2007) Morphology/behaviour relationship of nanocomposites based on natural rubber/epoxidized natural rubber blends. *Compos Sci Technol* 67:1330–1339. <https://doi.org/10.1016/j.compscitech.2006.09.019>
- Bhattacharya M (2016) Polymer nanocomposites—a comparison between carbon nanotubes, graphene, and clay as nanofillers. *Materials* 9:262. <https://doi.org/10.3390/ma9040262>
- Charoenchai M, Tangbunsuk S, Keawwattana W (2019) Influence of Graphene Nanoplatelets on silica-filled natural rubber composites: dispersion mixing and effect on thermal stability, rheological and mechanical properties. In: *Materials science forum*. Trans Tech Publ, pp 100–104. <https://doi.org/10.4028/www.scientific.net/MSF.943.100>
- Chen RS, Ab Ghani MH, Ahmad S, Salleh MN, Tarawneh MA (2015) Rice husk flour bio-composites based on recycled high-density polyethylene/polyethylene terephthalate blend: effect of high filler loading on physical, mechanical and thermal properties. *J Compos Mater* 49:1241–1253. <https://doi.org/10.1177/0021998314533361>
- Chen RS, Mohd Amran NA, Ahmad S (2018) Reinforcement effect of nanocomposites with single/hybrid graphene nanoplatelets and magnesium hydroxide. *J Therm Anal Calorim*. <https://doi.org/10.1007/s10973-018-7935-y>
- Das A, Kasaliwal GR, Jurk R, Boldt R, Fischer D, Stöckelhuber KW, Heinrich G (2012a) Rubber composites based on graphene nanoplatelets, expanded graphite, carbon nanotubes

- and their combination: a comparative study. *Compos Sci Technol* 72:1961–1967. <https://doi.org/10.1016/j.compscitech.2012.09.005>
- Das A et al (2012b) Rubber composites based on graphene nanoplatelets, expanded graphite, carbon nanotubes and their combination: a comparative study. 72:1961–1967
- Eleuteri M, Bernal M, Milanese M, Monticelli O, Fina A (2019) Stereocomplexation of poly(lactic acid)s on graphite Nanoplatelets: from functionalized nanoparticles to self-assembled nanostructures. *Front Chem* 7:176–176. <https://doi.org/10.3389/fchem.2019.00176>
- Fang M, Wang K, Lu H, Yang Y, Nutt S (2009) Covalent polymer functionalization of graphene nanosheets and mechanical properties of composites. *J Mater Chem A* 19:7098–7105. <https://doi.org/10.1039/B908220D>
- Ganguli S, Roy AK, Anderson, DP (2008) Improved thermal conductivity for chemically functionalized exfoliated graphite/epoxycomposites. *Carbon* 46:806–817. <https://doi.org/10.1016/j.carbon.2008.02.008>
- Ijeomah G, Samsuri F, Md Zawawi MA (2017) A review of surface engineering of Graphene for electrochemical sensing applications. *J Eng Technol* 8:1–31. <https://doi.org/10.15282/ijets.8.2017.1.1.1076>
- Jayalatha G, Kutty SK (2013) Effect of short nylon-6 fibres on natural rubber-toughened polystyrene. *Mater Des* 43:291–298. <https://doi.org/10.1016/j.matdes.2012.05.020>
- Karger-Kocsis J, Felhös D, Xu D (2010) Mechanical and tribological properties of rubber blends composed of HNBR and in situ produced polyurethane. *Wear* 268:464–472. <https://doi.org/10.1016/j.wear.2009.08.037>
- Kim H, Abdala AA, Macosko CW (2010) Graphene/polymer nanocomposites. *Macromolecules* 43:6515–6530. <https://doi.org/10.1021/ma100572e>
- Konar B, Roy S, Pariya T (2010) Study on the effect of nano and active particles of alumina on natural rubber–alumina composites in the presence of epoxidized natural rubber as compatibilizer. *J Macromol Sci Part A Pure Appl Chem*. 47:416–422. <https://doi.org/10.1080/10601321003659531>
- Kuan C-F, Chiang C-L, Lin S-H, Huang W-G, Hsieh W-Y, Shen M-Y (2018) Characterization and properties of Graphene nanoplatelets/XnBr nanocomposites. *Polym Polym Compos* 26:59–68. <https://doi.org/10.1177/096739111802600107>
- Kuila T, Bose S, Mishra AK, Khanra P, Kim NH, Lee JH (2012) Chemical functionalization of graphene and its applications. *Prog Mater Sci* 57:1061–1105. <https://doi.org/10.1016/j.pmatsci.2012.03.002>
- La DD et al (2018) A new approach of fabricating Graphene Nanoplates@natural rubber latex composite and its characteristics and mechanical properties. *J Carb Res* 4:50. <https://doi.org/10.3390/c4030050>
- Li S, Li Z, Burnett TL, Slater TJ, Hashimoto T, Young RJ (2017) Nanocomposites of graphene nanoplatelets in natural rubber: microstructure and mechanisms of reinforcement. *J Mater Sci* 52:9558–9572. <https://doi.org/10.1007/s10853-017-1144-0>
- Liu M, Papageorgiou DG, Li S, Lin K, Kinloch IA, Young RJ (2018) Micromechanics of reinforcement of a graphene-based thermoplastic elastomer nanocomposite. *Compos Part A Appl S* 110:84–92. <https://doi.org/10.1016/j.compositesa.2018.04.014>
- Ma J et al (2014) Development of polymer composites using modified, high-structural integrity graphene platelets. *Compos Sci Technol* 91:82–90. <https://doi.org/10.1016/j.compscitech.2013.11.017>
- Mohamad N et al (2017) Vibrational damping behaviors of graphene nanoplatelets reinforced NR/EPDM nanocomposites. *J Mech Eng Sci* 11:3274–3287. <https://doi.org/10.15282/jmes.11.4.2017.28.0294>
- Motaung TE, Luyt AS, Thomas S (2011) Morphology and properties of NR/EPDM rubber blends filled with small amounts of titania nanoparticles. *Polym Compos* 32:1289–1296. <https://doi.org/10.1002/pc.21150>

- Nabil H, Ismail H, Azura A (2013) Compounding, mechanical and morphological properties of carbon-black-filled natural rubber/recycled ethylene-propylene-diene-monomer (NR/R--EPDM) blends. *Polym Test* 32:385–393. <https://doi.org/10.1016/j.polymertesting.2012.11.003>
- Razak J et al (2017) Characterization on thermal and mechanical properties of non-covalent Polyethyleneimine wrapped on Graphene Nanoplatelets within NR/EPDM rubber blend Nanocomposites. *J Ad Manuf Technol (JAMT)* 11:85–100
- Razak JA, Ahmad SH, Ratnam CT, Mahamood MA, Yaakub J, Mohamad N (2015) Graphene Nanoplatelets-filled NR/EPDM rubber blend: effects of GNPs loading on blend process ability, mechanical properties and fracture morphology. *J Polymres* 9:43
- Razak JA et al (2014) The effects of covalent treated graphene nanoplatelets surface modification to cure characteristic, mechanical, physical and morphological properties of NR/EPDM rubber blend nanocomposites. *Adv Environ Biol*:3289–3299
- Sae-oui P, Sirisinha C, Thepsuwan U, Thapthong P (2007) Influence of accelerator type on properties of NR/EPDM blends. *Polym Test* 26:1062–1067. <https://doi.org/10.1016/j.polymertesting.2007.07.004>
- Shehata A, Afifi H, Darwish N, Mounir A (2006) Evaluation of the effect of polymeric compounds as compatibilizers for NR/EPDM blend. *Polym-Plast Technol Eng* 45:165–170. <https://doi.org/10.1080/03602550500373964>
- Shen J, Li N, Shi M, Hu Y, Ye M (2010) Covalent synthesis of organophilic chemically functionalized graphene sheets. *J Colloid Interface Sci* 348:377–383. <https://doi.org/10.1016/j.jcis.2010.04.055>
- Sridhar V, Lee I, Chun H, Park H (2013) Graphene reinforced biodegradable poly (3-hydroxybutyrate-co-4-hydroxybutyrate) nano-composites. *Express Polym Lett* 7
- Srivastava S, Mishra Y (2018) Nanocarbon reinforced rubber Nanocomposites: detailed insights about mechanical, dynamical mechanical properties, Payne, and Mullin effects. *J Nanomater* 8:945. <https://doi.org/10.3390/nano8110945>
- Stuart B (2005) Infrared spectroscopy. In: Kirk-Othmer encyclopedia of chemical technology. <https://doi.org/10.1002/0471238961.0914061810151405.a01.pub2>
- Tavakoli M, Katbab AA, Nazockdast H (2011) Effectiveness of maleic anhydride grafted EPDM rubber (EPDM-g-MAH) as Compatibilizer in NR/Organoclay Nanocomposites prepared by melt compounding. *J Macromol Sci Part B* 50:1270–1284. <https://doi.org/10.1080/00222348.2010.507439>
- Wang X, Xing W, Zhang P, Song L, Yang H, Hu Y (2012) Covalent functionalization of graphene with organosilane and its use as a reinforcement in epoxy composites. *Compos Sci Technol* 72:737–743. <https://doi.org/10.1016/j.compscitech.2012.01.027>
- Zhang G, Wang F, Dai J, Huang Z (2016) Effect of functionalization of graphene nanoplatelets on the mechanical and thermal properties of silicone rubber composites. *Materials* 9:92. <https://doi.org/10.3390/ma9020092>
- Zhang H-B, Zheng W-G, Yan Q, Jiang Z-G, Yu Z-Z (2012) The effect of surface chemistry of graphene on rheological and electrical properties of polymethylmethacrylate composites. *Carbon* 50:5117–5125. <https://doi.org/10.1016/j.carbon.2012.06.052>
- Zhao S, Xie S, Liu X, Shao X, Zhao Z, Xin Z, Li L (2018) Covalent hybrid of graphene and silicon dioxide and reinforcing effect in rubber composites. *J Polym Res* 25:225. <https://doi.org/10.1007/s10965-018-1616-1>